J|A|C|S
ARTICLES
Published on Web 04/19/2002

Syntheses, Structures, and Surface Aromaticity of the New Carbaalane $[(AlH)_6(AlNMe_3)_2(CCH_2R)_6]$ (R = Ph, CH_2SiMe_3) and a Stepwise Functionalization of the Inner and Outer Sphere of the Cluster†

Andreas Stasch, Marilena Ferbinteanu,‡ Jörg Prust, Wenjun Zheng, Fanica Cimpoesu,§ Herbert W. Roesky,* Jörg Magull, Hans-Georg Schmidt, and Mathias Noltemeyer

Contribution from the Institut für Anorganische Chemie der Georg-August-Universität Göttingen, Tammannstrasse 4, 37077 Göttingen, Germany

Received August 23, 2001

Abstract: The reaction of the acetylene RC≡CH (R = Ph, CH_2SiMe_3) with an excess of $AlH_3{\cdot}NMe_3$ in boiling toluene leads to the carbaalane $[(AlH)_6(AlNMe_3)_2(CCH_2R)_6]$ (R = Ph **1**, CH_2SiMe_3 **2**) in good yield. Treatment of **2** with BCl_3 under varying conditions gives the chlorinated products $[(AlCl)_6(AlNMe_3)_2(CCH_2CH_2SiMe_3)_6]$ **3** and $[(AlCl)_6(AlNMe_3)_2(CCH_2CH_2SiMe_2Cl)_6]$ **4**, respectively. The latter clearly demonstrates that the cluster can be stepwise functionalized within the inner and outer sphere. The X-ray single-crystal structures of **1**, **2**, and **4** have been determined. All compounds have in common that the central core consists of a cluster having eight aluminum and six carbon atoms. The bonding properties in this cluster are described as a new manifestation of three-dimensional surface aromaticity. Each Al_4C fragment of the cube is formed by four bonds with three electron pairs, thus leading to a strong delocalization of the electrons. A phenomenological modeling using a three-dimensional Hückel scheme with fitted parameters to reproduce the energies from ab initio calculations revealed that the orbital scheme localized at one Al_4C fragment possesses an orbital sextet with a large HOMO−LUMO gap. This is in line with the criteria of aromaticity. The idea of aromaticity was sustained also by qualitative valence bond reasons enumerating the different resonance structures by means of graph theoretical methods.

1. Introduction

Hydroalumination is an important reaction on a large industrial[1] scale and in the laboratory.[2] Although it is widely used, only few publications deal with the hydroalumination products.[3] In most reactions, the organic component is released by hydrolysis. Carbaalanes are known since 1999 and have been established along with carbaboranes (carboranes) as a new and interesting class of compounds.[4] They were synthesized by Uhl et al. from substituted aluminum acetylides and dialkylaluminum hydrides. Recently, we reported on reactions of monosubstituted acetylenes with dimeric pyrazolato aluminum dihydrides leading for the first time to terminal aluminum acetylides.[5] Those compounds show an interesting chemical behavior. Therefore, we decided to extend these investigations on hydride-rich aluminum derivatives to synthesize hydroalumination products. Very recently, we were successful in synthesizing polyhedral aluminum compounds by hydroalumination of nitriles and isonitriles with $AlH_3{\cdot}NMe_3$.[6]

† These compounds are named cluster although metal−metal bonds do not exist.

* To whom correspondence should be addressed. Fax: (+49)551-39-3373. E-mail: hroesky@gwdg.de.

‡ Permanent address: University of Bucharest, Faculty of Chemistry, Inorganic Chemistry Department, Dumbrava Rosie 23, Bucharest 70254, Romania. E-mail: mcimpoesu@yahoo.com.

§ Institute of Physical Chemistry, Splaiul Independentei 202, 77208 Bucharest, Romania.

(1) First investigations and technical applications: (a) Ziegler, K. *Angew. Chem.* **1952**, *64*, 323−329. (b) Ziegler, K.; Gellert, H.-G.; Martin, H.; Nagel, K. *Justus Liebigs Ann. Chem.* **1954**, *589*, 91−121. (c) Ziegler, K.; Gellert, H.-G.; Zosel, K.; Lehmkuhl, W.; Pfohl, W. *Angew. Chem.* **1955**, *67*, 424. (d) Ziegler, K. *Angew. Chem.* **1956**, *68*, 721−729. (e) Ziegler, K.; Gellert, H.-G.; Lehmkuhl, H.; Pfohl, W.; Zosel, K. *Justus Liebigs Ann. Chem.* **1960**, *629*, 1−13.

(2) Examples for organic syntheses: (a) Winterfeldt, E. *Synthesis* **1975**, 617−630. (b) Marek, I.; Normant, J.-F. *Chem. Rev.* **1996**, *96*, 3241−3267.

(3) Examples for hydroalumination products: (a) Dümichen, U.; Thiele, K.-H.; Gelbrich, T.; Sieler, J. *J. Organomet. Chem.* **1995**, *495*, 71−75. (b) Gardiner, M. G.; Lawrence, S. M.; Raston, C. L. *Inorg. Chem.* **1995**, *34*, 4652−4659. (c) Francis, J. A.; Bott, S. G.; Barron, A. R. *Main Group Chem.* **1999**, *3*, 53−57. (d) Uhl, W.; Breher, F. *J. Organomet. Chem.* **2000**, *608*, 54−59.

(4) (a) Uhl, W.; Breher, F. *Angew. Chem.* **1999**, *111*, 1578−1580; *Angew. Chem., Int. Ed.* **1999**, *38*, 1477−1479. (b) Uhl, W.; Breher, F. *Eur. J. Inorg. Chem.* **2000**, 1−11. (c) Uhl, W.; Breher, F.; Lützen, A.; Saak, W. *Angew. Chem.* **2000**, *112*, 414−416; *Angew. Chem., Int. Ed.* **2000**, *39*, 406−409. (d) Uhl, W.; Breher, F. *Organometallics* **2000**, *19*, 4536−4543. (e) Uhl, W.; Breher, F.; Mbonimana, A.; Gauss, J.; Haase, D.; Lützen, A.; Saak, W. *Eur. J. Inorg. Chem.* **2001**, 3059−3066.

(5) (a) Zheng, W.; Mösch-Zanetti, N. C.; Roesky, H. W.; Hewitt, M.; Cimpoesu, F.; Schneider, T. R.; Stasch, A.; Prust, J. *Angew. Chem.* **2000**, *112*, 3099−3101; *Angew. Chem., Int. Ed.* **2000**, *39*, 3127−3130. (b) Zheng, W.; Hohmeister, H.; Mösch-Zanetti, N. C.; Roesky, H. W.; Noltemeyer, M.; Schmidt, H.-G. *Inorg. Chem.* **2001**, *40*, 2363−2366.

(6) (a) Zheng, W.; Stasch, A.; Prust, J.; Roesky, H. W.; Cimpoesu, F.; Noltemeyer, M.; Schmidt, H.-G. *Angew. Chem.* **2001**, *113*, 3569−3572; *Angew. Chem., Int. Ed.* **2001**, *40*, 3461−3464. (b) Reddy, N. D.; Roesky, H. W.; Noltemeyer, M.; Schmidt, H.-G. *Inorg. Chem.* **2002**, *41*, in press.

Table 1. Crystal Data and Experimental Parameters for the Crystal Structure Analyses of **1**(·2 Toluene), **2**(·2 Toluene), and **4**(·6 Toluene)

	1(·2C_7H_8)	**2**(·2C_7H_8)	**4**(·6C_7H_8)
empirical formula	$C_{68}H_{82}Al_8N_2$	$C_{56}H_{118}Al_8N_2Si_6$	$C_{78}H_{126}Al_8Cl_{12}N_2Si_6$
formula weight, g mol^{-1}	1143.20	1203.90	1901.59
T, K	293(2)	200(2)	133(2)
λ (Mo Kα), Å	0.71073	0.71073	0.71073
crystal system	triclinic	monoclinic	monoclinic
space group	$P-1$	$P2(1)/c$	$C2/c$
a, Å	11.527(2)	12.906(3)	32.3959(13)
b, Å	11.961(2)	12.544(3)	15.9888(9)
c, Å	12.761(3)	24.554(5)	23.8710(10)
α, deg	105.54(3)	90	90
β, deg	100.88(3)	91.14(3)	124.744(4)
γ, deg	101.67(3)	90	90
V, Å^3	1604.1(6)	3974.1(14)	10 160.0(8)
Z	1	2	4
ρ_{calc}, Mg m^{-3}	1.183	1.006	1.243
absorption coefficient, mm^{-1}	0.169	0.224	0.506
crystal size, mm	0.80 × 0.60 × 0.60	0.60 × 0.50 × 0.40	0.30 × 0.30 × 0.30
F (000)	608	1312	4000
θ range, deg	3.52−25.03	3.54−25.00	1.49−24.72
index ranges	$-13 \le h \le 13$, $-14 \le k \le 13$, $-15 \le l \le 15$	$-15 \le h \le 15$, $-14 \le k \le 14$, $-29 \le l \le 29$	$-37 \le h \le 38$, $-18 \le k \le 18$, $-28 \le l \le 26$
reflections collected	6586	12 465	29 829
unique	5419	6980	8316
R_{int}	0.2933	0.0597	0.0738
completeness to θ	95.4%	99.7%	96.1%
refinement method	full-matrix least squares on F^2	full-matrix least squares on F^2	full-matrix least squares on F^2
diffractometer	Stoe−Siemens−Huber	Stoe−Siemens−Huber	Stoe IPDS II-
data/restraints/parameters	5419/3/366	6980/439/334	8316/0/437
GOF on F^2	1.037	1.033	1.066
final R indices [$I > 2\sigma(I)$]	$R_1 = 0.0763$, w$R_2 = 0.1645$	$R_1 = 0.0494$, w$R_2 = 0.1225$	$R_1 = 0.0506$, w$R_2 = 0.1434$
R indices (all data)	$R_1 = 0.1461$, w$R_2 = 0.2045$	$R_1 = 0.0691$, w$R_2 = 0.1363$	$R_1 = 0.0615$, w$R_2 = 0.1486$
largest difference peak and hole, e Å^{-3}	0.753 and −0.329	0.516 and −0.344	1.142 and −0.474

2. Experimental Section

2.1. General Procedures. All manipulations were performed under a dry and oxygen-free nitrogen atmosphere using standard Schlenk and glovebox techniques. All solvents were dried appropriately, distilled, and degassed prior to use.

Crystallographic data are summarized in Table 1. The data for **1** and **2** were collected on a Stoe−Siemens−Huber four-circle diffractometer coupled to a Siemens CCD area-detector and for **4** on a Stoe IPDS II-array detector system instrument in both cases with graphite-monochromated Mo Kα radiation ($\lambda = 0.71073$ Å). The structures were solved by direct methods and were refined using SHELX-97.[7]

The Gaussian 98[8] and GAMESS[9] computer program packages were used for ab initio calculations.

2.2. Synthesis of [(AlH)$_6$(AlNMe$_3$)$_2$(CCH$_2$Ph)$_6$] (1). Phenylacetylene (0.47 g, 0.50 mL, 4.55 mmol, 1 equiv) was added to a solution of AlH_3·NMe_3[10] (27.3 mL of a 0.5 M solution in toluene, 13.7 mmol, 3 equiv) in toluene (25 mL) and stirred for 1 h at room temperature. The reaction mixture was heated under reflux for 30 min. First, gas evolution was observed, and the color turned red followed by decolorization after 15 min. A precipitate was filtered off, and the solution was stored at 4 °C to form colorless single crystals of **1** (·2 toluene) for X-ray structural analysis. The solution was reduced in vacuo to 20 mL and crystallized at −24 °C. The obtained crystals were dried in vacuo. Yield: 0.62 g of **1** (0.65 mmol, 85%), mp 280−282 °C (decomp). ^{1}H NMR (200 MHz, C_6D_6, 296 K, TMS): $\delta = 2.04$ (s, 12H, CH_2), 2.10 (s, 18H, N(CH_3)$_3$), 4.0 (s, very broad, 6H, Al*H*), 6.96−7.15 (m, 30H, Ph*H*). EI-MS (70 eV): The mass spectrum only provided CH fragments. IR (Nujol): $\tilde{\nu} = 1822$ (Al−H), 1262, 1091, 1029, 976, 802, 756, 721, 681, 563, 509 cm^{-1}. Anal. Calcd for $C_{54}H_{66}Al_8N_2$ (958.97): C, 67.63; H, 6.94; N, 2.92. Found: C, 66.40; H, 6.95; N, 2.90.

For Preparative Uses: A solution of AlH_3·NMe_3 (100 mL of a 0.5 M solution in toluene, 50 mmol, 3 equiv) and phenylacetylene (1.70 g, 1.83 mL, 16.7 mmol, 1 equiv) was heated for 1 h under reflux. The reaction mixture was reduced in vacuo to 20 mL. *n*-Hexane (30 mL) was added and stirred for 1 h at −30 °C. The precipitate was filtered off, washed with *n*-hexane (20 mL), and dried in vacuo for 6 h at 35 °C. Yield: 2.53 g of **1** (15.8 mmol, 95%, purity[11] > 95%).

2.3. Synthesis of [(AlH)$_6$(AlNMe$_3$)$_2$(CCH$_2$CH$_2$SiMe$_3$)$_6$] (2). A solution of $Me_3SiCH_2C{\equiv}CH$[12] (1.00 g, 1.33 mL, 8.91 mmol, 1 equiv) and AlH_3·NMe_3 (40 mL of a 0.7 M solution in toluene, 28.0 mmol, 3.14 equiv) was heated under reflux for 45 min. The reaction mixture

(7) Sheldrick, G. M. *SHELX-97*, Programs for Crystal Structure Refinement; Universität Göttingen, 1997.
(8) The 6-311G* basis was used; the DFT calculations were based on B3LYP and BWVN functionals; calculation perfomed with: Frisch, M. J.; Trucks, G. W.; Schlegel, H. B.; Scuseria, G. E.; Robb, M. A.; Cheeseman, J. R.; Zakrzewski, V. G.; Montgomery, J. A., Jr.; Stratmann, R. E.; Burant, J. C.; Dapprich, S.; Millam, J. M.; Daniels, A. D.; Kudin, K. N.; Strain, M. C.; Farkas, O.; Tomasi, J.; Barone, V.; Cossi, M.; Cammi, R.; Mennucci, B.; Pomelli, C.; Adamo, C.; Clifford, S.; Ochterski, J.; Petersson, G. A.; Ayala, P. Y.; Cui, Q.; Morokuma, K.; Malick, D. K.; Rabuck, A. D.; Raghavachari, K.; Foresman, J. B.; Cioslowski, J.; Ortiz, J. V.; Stefanov, B. B.; Liu, G.; Liashenko, A.; Piskorz, P.; Komaromi, I.; Gomperts, R.; Martin, R. L.; Fox, D. J.; Keith, T.; Al-Laham, M. A.; Peng, C. Y.; Nanayakkara, A.; Gonzalez, C.; Challacombe, M.; Gill, P. M. W.; Johnson, B. G.; Chen, W.; Wong, M. W.; Andres, J. L.; Head-Gordon, M.; Replogle, E. S.; Pople, J. A. *Gaussian 98*, revision A.6; Gaussian, Inc.: Pittsburgh, PA, 1998.
(9) The RHF calculation was carried out with the GAMESS package: Schmidt, M. W.; Baldridge, K. K.; Boatz, J. A.; Elbert, S. T.; Gordon, M. S.; Jensen, J. H.; Koseki, S.; Matsunaga, N.; Nguyen, K. A.; Su, S. J.; Windus, T. L.; Dupuis, M.; Montgomery, J. A. *J. Comput. Chem.* **1993**, *14*, 1347−1363.
(10) (a) Wiberg, E.; Graf, H.; Uson, R. *Z. Anorg. Allg. Chem.* **1953**, *272*, 221−232. (b) Kovar, R. A.; Callaway, J. O. *Inorg. Synth.* **1975**, *17*, 36−40.
(11) A minor impurity of AlH_3·NMe_3 leads to the formation of aluminum metal from the decomposition reaction which occurs at high temperature (refluxing in toluene >1 h) or storage at room temperature (>1 week). See: (a) Fooken, U.; Khan, M. A.; Wehmschulte, R. J. *Inorg. Chem.* **2001**, *40*, 1316−1322. (b) Stecher, O.; Wiberg, E. *Ber. Dtsch. Chem. Ges.* **1942**, *75*, 2003−2012.
(12) The propargyl-trimethylsilane shows an equilibrium with the corresponding allenyl-trimethylsilane (ca 10−15%): Slutsky, J.; Kwart, H. *J. Am. Chem. Soc.* **1973**, *95*, 8678−8685.

was reduced in vacuo to 10 mL and stored at 4 °C to form colorless blocks of **2**·2 toluene. The solution was removed using a syringe and crystallized at −24 °C. Yield: 1.65 g of **2** (·2 toluene), (1.38 mmol, 93%), mp 242−244 °C (decomp). Toluene NMR resonances are not given. ^{1}H NMR (200 MHz, C_6D_6, 296 K, TMS): δ = 0.06 (s, 54H, Si(CH_3)$_3$), 1.46 (ddd, J = 9.1, 4.3, 4.3 Hz, 12H, Me$_3$SiCH_2), 2.10 (s, 18H, N(CH_3)$_3$), 2.25 (ddd, J = 9.1, 4.3, 4.3 Hz, 12H, CH_2C), 5.0 (s, very broad, 6H, AlH). ^{13}C{^{1}H} NMR (126 MHz, C_6D_6, 296 K, TMS): δ = −1.46 (Si(*C*H$_3$)$_3$), 16.8 (cluster *C*), 26.0 (Me$_3$Si*C*H$_2$), 27.3 (*C*H$_2$C), 46.6 (N(*C*H$_3$)$_3$). ^{27}Al NMR (65.2 MHz, C_6D_6, 296 K, Al(H$_2$O)$_6^{3+}$): δ = 142.3 (s, $W_{1/2} \approx$ 2500 Hz). ^{29}Si{^{1}H} NMR (99.4 MHz, C_6D_6, 296 K, TMS): δ = −0.22. EI-MS (70 eV) *m*/*z* (%): 1176.6, 1032.6 (2) [(M + CH$_2$)$^+$], 1018.6 (13) [M$^+$], 1004.5 (2) [(M − CH$_2$)$^+$], 989.6 (2) [(M − C$_2$H$_5$)$^+$], 959.5 (2) [(M − NMe$_3$)$^+$], 945.4 (1) [(M − SiMe$_3$)$^+$], 101.1 (17) [Me$_3$SiC$_2$H$_4^+$], 73.0 (100) [Me$_3$Si$^+$]. IR (Nujol): $\tilde{\nu}$ = 1802 (Al−H), 1770 (Al−H), 1311, 1245, 1172, 1019, 963, 915, 865, 834, 769, 724, 690, 658, 633, 557 cm^{-1}. Anal. Calcd for $C_{42}H_{102}Al_8N_2Si_6$ (·2C_7H_8) (1203.91): C, 55.87; H, 9.88; N, 2.33. Found: C, 53.94; H, 9.91; N, 2.42.

2.4. Synthesis of [(AlCl)$_6$(AlNMe$_3$)$_2$(CCH$_2$CH$_2$SiMe$_3$)$_6$] (3). BCl$_3$ (0.76 mL of a 1 M solution in *n*-hexane, 2.05 equiv) was added dropwise to a solution of **2** (0.38 g, 0.37 mmol, 1 equiv) in toluene (15 mL) at −78 °C and stirred for 0.5 h at this temperature. The reaction mixture was further stirred for 0.5 h at 0 °C and 2 h at room temperature. All volatiles were removed in vacuo at 30 °C, and the residue was recrystallized from toluene (ca. 5 mL, 50 °C/4 °C) to form light yellow blocks. The crystals were dried in vacuo. Yield: 0.38 g of **3** (0.31 mmol, 84%), mp 233 °C (decomp). For further preparations, the crude product does not need to be recrystallized (yield 100%). ^{1}H NMR (500 MHz, C_6D_6, 296 K, TMS): δ = 0.08 (s, 54H, Si(CH_3)$_3$), 1.53 (ddd, J = 9.1, 4.3, 4.3 Hz, 12H, Me$_3$SiCH_2), 2.25 (s, 18H, N(CH_3)$_3$), 2.36 (ddd, J = 9.1, 4.3, 4.3 Hz, 12H, CH_2C). ^{13}C{^{1}H} NMR (126 MHz, C_6D_6, 296 K, TMS): δ = −1.59 (Si(*C*H$_3$)$_3$), 25.8 (Me$_3$Si*C*H$_2$), 28.1 (*C*H$_2$C), 32.1 (cluster *C*), 48.2 (N(*C*H$_3$)$_3$). ^{27}Al NMR (65.2 MHz, C_6D_6, 296 K, Al(H$_2$O)$_6^{3+}$): δ = 140.9 (s, $W_{1/2}$ = 750 Hz). ^{29}Si{^{1}H} NMR (99.4 MHz, C_6D_6, 296 K, TMS): δ = 0.2. EI-MS (70 eV) *m*/*z* (%): 1226.2 [M$^+$]. IR (Nujol): $\tilde{\nu}$ = 1268, 1086, 1022, 802, 728, 605 cm^{-1}. Anal. Calcd for $C_{42}H_{96}Al_8Cl_6N_2Si_6$ (1226.31): C, 41.14; H, 7.89; N, 2.28. Found: C, 42.78; H, 7.90; N, 2.25.

2.5. Synthesis of [(AlCl)$_6$(AlNMe$_3$)$_2$(CCH$_2$CH$_2$SiMe$_2$Cl)$_6$] (4). BCl$_3$ (12.0 mL of a 1 M solution in *n*-hexane, 44 equiv) was added dropwise to a solution of **2** (0.28 g, 0.27 mmol, 1 equiv) in toluene (20 mL) at −78 °C and stirred for 3 d at room temperature. The reaction mixture was heated under reflux for 1 h, and all volatiles were removed in vacuo at 35 °C. The residue was recrystallized from toluene (ca. 3 mL, 60 °C/room temperature) to form light green blocks. Yield: 0.41 g of **4** (·6 toluene), (0.21 mmol, 78%), mp 188 °C (decomp). Toluene NMR resonances are not given. ^{1}H NMR (200 MHz, C_6D_6, 296 K, TMS): δ = 0.28 (s, 36H, Si(CH_3)$_2$), 1.73 (ddd, J = 9.1, 4.3, 4.3 Hz, 12H, Me$_2$ClSiCH_2), 2.34 (s, 18H, N(CH_3)$_3$), 2.54 (ddd, J = 9.1, 4.3, 4.3 Hz, 12H, CH_2C). ^{13}C{^{1}H} NMR (126 MHz, C_6D_6, 296 K, TMS): δ = 1.54 (Si(*C*H$_3$)$_2$), 24.5 (Me$_2$ClSi*C*H$_2$), 28.9 (*C*H$_2$C), 30.2 (cluster *C*), 48.3 (N(*C*H$_3$)$_3$). ^{27}Al NMR (65.2 MHz, C_6D_6, 296 K, Al(H$_2$O)$_6^{3+}$): δ = 141.4 (s, $W_{1/2}$ = 850 Hz). ^{29}Si{^{1}H} NMR (99.4 MHz, C_6D_6, 296 K, TMS): δ = −21.5. EI-MS (70 eV) *m*/*z* (%): 1348.0 [M$^+$]. IR (Nujol): $\tilde{\nu}$ = 1264, 1100, 1016, 800, 725 cm^{-1}. Anal. Calcd for $C_{36}H_{78}Al_8Cl_{12}N_2Si_6$ (·6C_7H_8) (1901.65): C, 49.26; H, 6.68; N, 1.47. Found: C, 48.12; H, 6.48; N, 1.53.

3. Results and Discussion

3.1. Preparation of 1 and 2. Treatment of the acetylene RC≡CH (R = Ph, CH$_2$SiMe$_3$[12]) with an excess of the alane trimethylamine adduct[10] in boiling toluene leads to the formation of the carbaalane [(AlH)$_6$(AlNMe$_3$)$_2$(CCH$_2$R)$_6$] (R = Ph **1**, CH$_2$SiMe$_3$ **2**) in good yields (Scheme 1). During the reaction, gas evolution can be noticed. In the case of the formation of **1**, the reaction mixture turns red after a few minutes of refluxing, and later on decolorization is observed. The reaction mixture for the preparation of **2** is colorless at any time. At elevated temperatures, the acetylene hydrogen atom is deprotonated by an aluminum hydride, and two aluminum hydride bonds are regioselectively added to the C≡C triple bond. This leads to a RCH$_2$C-group (R = Ph (**1**), CH$_2$SiMe$_3$ (**2**)) and the carbon atom connected to the aluminum atoms forming the cluster. Colorless crystals of **1** (·2 toluene) and **2** (·2 toluene) can be recovered in good yield from the reaction mixture.

Scheme 1

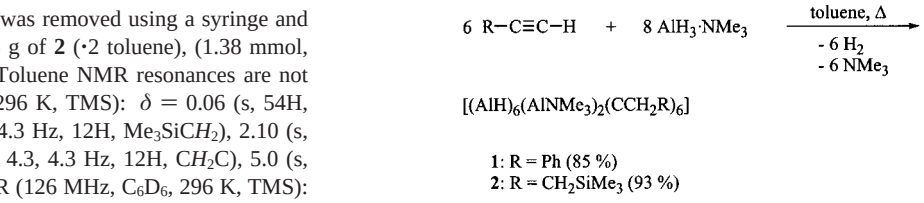

The corresponding reaction with the silylacetylene R$_3$SiC≡CH (R = Me, Ph) does not lead to specific carbaalanes. NMR investigations indicate that nonregioselective hydroalumination leads to a mixture of products. No pure compounds could be separated from the reaction mixtures.

3.2. X-ray Crystal Structure Analyses of 1 and 2. Compounds **1** and **2** crystallize with two molecules of toluene in the triclinic *P*-1 and monoclinic space group *P*2(1)/*c*, respectively. The molecular structures of **1** and **2** are depicted in Figures 1 and 2. The central framework of **1** and **2** is a rhombic dodecahedron containing a cube of eight aluminum atoms with six carbon atoms attached to the Al$_4$ planes of the cube, bearing the organic groups. Six aluminum atoms carry a hydrogen atom, whereas two aluminum atoms on opposite sides of the cluster (in 1,4 position) are each bearing a trimethylamine ligand. Each cluster carbon atom is connected with three AlH and one Al(NMe$_3$) unit. The result is a closed carbaalane cluster with a nearly D_{3h} symmetry. As expected, the average bond distances from Al(NMe$_3$) atoms to the closest cluster carbon atoms (2.028 Å (**1**), 2.024 Å (**2**)) are shorter than the corresponding distances from AlH atoms to the cluster carbon atoms (2.095 Å (**1**), 2.086 Å (**2**)). The average bond distance between Al(NMe$_3$) and AlH atoms (2.584 Å (**1**), 2.583 Å (**2**)) is somewhat shorter than the corresponding AlH−AlH distance (2.644 Å (**1**), 2.614 Å (**2**)). The Al−Al bond distances are comparable with those in dimeric trimethylaluminum[13] (2.606(2) Å) and in the published carbaalanes.[4] The average Al−C−Al angles are 78.34 and 127.10° for **1** (77.41 and 125.77° for **2**), whereas the AlH−C−AlH and Al(NMe$_3$)−C−AlH units have angles of 77.50, 123.90° for **1** and 77.91, 124.08° for **2**, respectively.

3.3. Spectroscopic Data of 1 and 2. The NMR spectra of **1** and **2** are in agreement with a highly symmetric structure. The ^{1}H NMR resonances of the methylene group connected to the cluster carbon atoms are found at δ 2.04 (s) for **1** and at δ 2.25 (ddd) for **2**. They resonate in the high field region comparable with those of the previously characterized carbaalanes (δ 2.0−3.4).[4] This is also observed for the ^{13}C NMR resonance of the cluster carbon atoms of **2** (δ 16.8) which is also found at high

(13) (a) Vranka, R. G.; Amma, E. L. *J. Am. Chem. Soc.* **1967**, *89*, 3121−3126. (b) Huffman, J. C.; Streib, W. E. *J. Chem. Soc., Chem. Commun.* **1971**, 911−912.

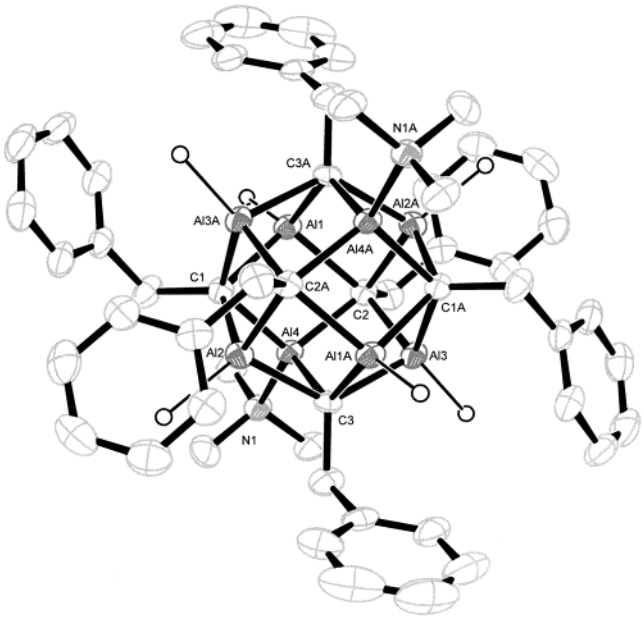

Figure 1. Molecular structure of **1**·2C_7H_8. Toluene molecules are omitted for clarity. Only hydrogen atoms bound to aluminum are depicted. Selected bond distances [Å] and angles [deg], average values in brackets: Al(NMe_3)−C(cluster) from 2.025(5) to 2.034(5) (2.028), Al(H)−C(cluster) from 2.079(5) to 2.106(5) (2.095), Al(NMe_3)−Al(H) from 2.578(2) to 2.592(2) (2.584), Al(H)−Al(H) from 2.641(2) to 2.648(2) (2.644), C(cluster)−CH_2-Ph from 1.568(7) to 1.586(7) (1.576), Al−H (1.886); Al(H)−C(cluster)−Al(H) from 78.20(18) to 78.51(18) (78.34) and from 127.0(3) to 127.2(2) (127.1), Al(NMe_3)−C(cluster)−Al(H) from 77.00(19) to 77.7(2) (77.50) and from 123.8(3) to 124.0(3) (123.9), C(cluster)−Al(NMe_3)−C(cluster) from 103.5(2) to 104.0(2) (103.7), C(cluster)−Al(H)−C(cluster) from 98.6(2) to 99.8(2) (99.26), Al(H)−Al(H)−Al(H) from 90.44(7) to 90.79(8) (90.66), Al(H)−Al(H)−Al(NMe_3) from 87.75(8) to 88.24(8) (87.97), Al(H)−Al(NMe_3)−Al(H) from 93.24(8) to 93.52(8) (93.38).

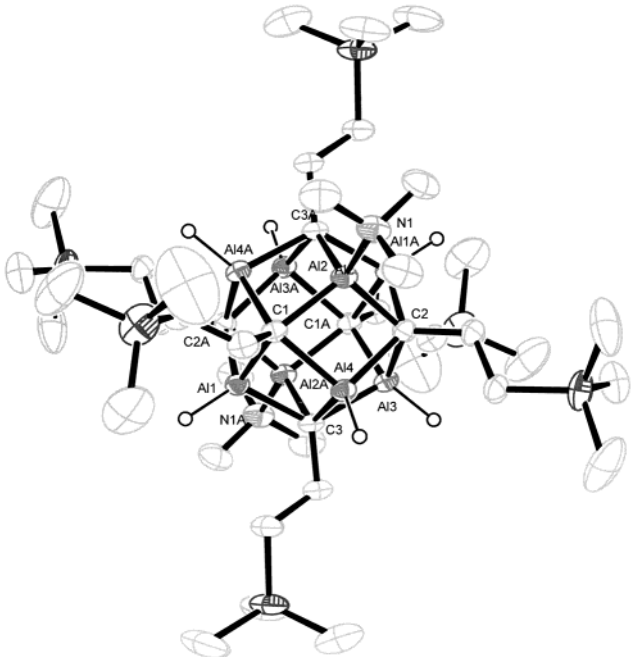

Figure 2. Molecular structure of **2**·2C_7H_8. Toluene molecules are omitted for clarity. Selected bond distances (av) [Å] and angles [deg]: Al(NMe_3)−C(cluster) 2.024, Al(H)−C(cluster) 2.086, Al(NMe_3)−Al(H) 2.583, Al(H)−Al(H) 2.614; Al(H)−C(cluster)−Al(H) 77.41 and 125.77, Al(NMe_3)−C(cluster)−Al(H) 77.91 and 124.08.

field range as compared to previous systems (δ 15.4−35.1).[4] Although there are two aluminum atoms of different environments (3:1), only one broad resonance (δ 142.3) is exhibited in the ^{27}Al NMR spectrum of **2**. Because of the very poor solubility of **1** in benzene and THF, no ^{13}C and ^{27}Al NMR resonances could be detected. A moderate solubility can only be achieved in boiling toluene. The aluminum hydride stretching frequencies can be found in the IR spectrum ($\tilde{\nu}$ = 1822 cm^{-1} (broad) for **1**, $\tilde{\nu}$ = 1802 and 1770 cm^{-1} for **2**). The mass spectrum (EI) of **1** only provides CH fragments, while for **2**, the molecular ion (m/z = 1018.6 M^+, 13%) and several fragments could be detected in the correct isotopic pattern.

Scheme 2

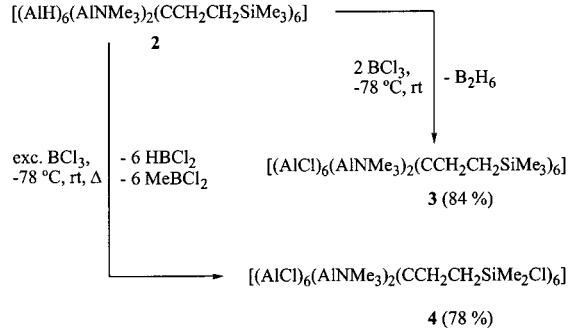

3.4. Preparation of 3 and 4. Compound **2** is well soluble in toluene and shows a high crystallization ability. Therefore, this compound is suitable for further reactions. Organo aluminum halides are important precursors for substitution reactions. They are mostly synthesized by salt elimination reactions from metalated organic ligands and aluminum halides. For the products obtained by hydroalumination reactions, the Al−H functionalities must be converted to an Al−X (X = halogen) group. This was realized with HgX_2 (X = Cl, Br, I),[14] HX (X = F, Cl, Br),[15] Me_3SiX (X = Cl, Br),[16] and X_2 (X = Br, I)[5b,15b] to form products with Al−X bonds. Treatment of **2** with 2 equiv of BCl_3 in toluene/*n*-hexane at low temperature and stirring for 1 day at room temperature yields compound **3** and B_2H_6 (Scheme 2). When **2** is reacted with an excess of BCl_3 in toluene/*n*-hexane at room temperature and heated for 1 h, no cleavage of the cluster core and no formation of $AlCl_3$ are observed. Instead, compound **4** containing 12 chlorine atoms is formed. Under these conditions, six Al−H are converted to six Al−Cl units, and all $SiMe_3$ groups of the ligand yield chemoselectively the $SiMe_2Cl$ moiety. Recrystallization from warm toluene afforded light yellow crystals of **3** and light green blocks of **4** (·6 toluene). This experiment clearly demonstrates that the cluster can be stepwise functionalized within the inner and outer sphere. The Al_8C_6 core is not degradated during this transformation, thus reflecting the stability of the cluster core. The easy access of compounds **3** and **4** shows for the first time that simultaneously a chemistry at the core as well as at the periphery can be developed.

3.5. X-ray Crystal Structure Analyses of 4. The X-ray single-crystal structure of **3** could not be determined due to poor crystal quality. Compound **4** crystallizes in the monoclinic space group *C*2/*c*. The molecular structure of **4** is depicted in Figure

(14) Nöth, H.; Wolfgardt, P. *Z. Naturforsch.* **1976**, *31B*, 697−708.
(15) (a) Avent, A. G.; Chen, W.-Y.; Eaborn, C.; Gorrell, I. B.; Hitchcock, P. B.; Smith, J. D. *Organometallics* **1996**, *15*, 4343−4345. (b) Al-Juaid, S. S.; Eaborn, C.; Gorrell, I. B.; Hawkes, S. A.; Hitchcock, P. B.; Smith, J. D. *J. Chem. Soc., Dalton Trans.* **1998**, 2411−2415.
(16) (a) Wehmschulte, R. J.; Power, P. P. *Inorg. Chem.* **1996**, *35*, 3262−3267. (b) Wehmschulte, R. J.; Power, P. P. *Polyhedron* **2000**, *19*, 1649−1661.

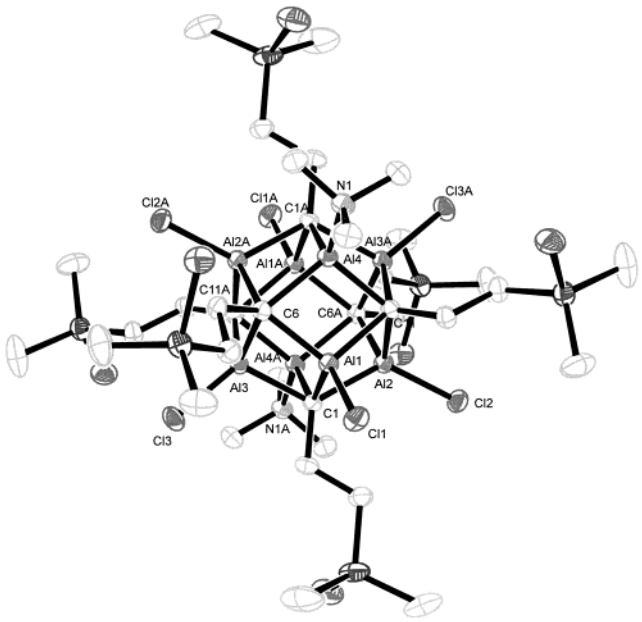

Figure 3. Molecular structure of **4**·6C$_7$H$_8$. Toluene molecules are omitted for clarity. Selected bond distances (av) [Å] and angles [deg]: Al−Cl 2.128, Al(NMe$_3$)−C(cluster) 2.051, Al(Cl)−C(cluster) 2.075, Al(NMe$_3$)−Al(Cl) 2.585, Al(Cl)−Al(H) 2.586; Al(Cl)−C(cluster)−Al(Cl) 77.03 and 124.30, Al(NMe$_3$)−C(cluster)−Al(Cl) 77.70 and 124.14.

3. The cluster core of **4** is comparable to that of **1**. The average Al−Cl bond length is 2.128 Å. The difference of the average bond length between Al(NMe$_3$)−C (2.051 Å) and Al(Cl)−C (2.075 Å) of **4** (0.024 Å) is not as big as the corresponding bond length difference between Al(NMe$_3$)−C (2.028 Å) and Al(H)−C (2.095 Å) of **1** (0.067 Å). The average Al−Al distance of **4** shows no differences between those of Al(Cl)−Al(Cl) (2.586 Å) and those of Al(NMe$_3$)−Al(Cl) (2.585 Å). Altogether, the cluster core of **4** is more symmetric than that of **1** and **2**.

3.6. Spectroscopic Data of 3 and 4. The ^{1}H NMR resonances of the methylene group connected to the cluster carbon atoms (ddd) are located at δ 2.36 and δ 2.54 for **3** and **4**, respectively. The ^{13}C NMR resonances of the cluster carbon atoms are found at δ 32.1 (**3**) and δ 30.2 (**4**). These resonances are shifted to lower field as compared with those of **1** and **2**. The ^{27}Al NMR resonances (δ 140.9 (**3**) and δ 141.4 (**4**)) show no significant changes as compared to **2**. The ^{29}Si NMR resonances are in agreement with Me$_3$Si (δ 0.2 (**3**)) and with a Me$_2$ClSi group (δ −21.5 (**4**)), respectively. The mass spectra of **3** and **4** show clearly the peaks of the molecular ions at m/z = 1226.2 (18%) and m/z = 1348.0 (2%), respectively, in the correct and characteristic isotopic pattern.

The ^{13}C NMR resonances of the cluster carbon atoms of **2** (δ 16.8), **3** (δ 32.1), and **4** (δ 30.2) are shifted to lower field as compared to organo aluminum compounds, but they are shifted to higher field as compared with benzene (δ 128). Obviously, the ^{13}C NMR resonances are in the same range as those of saturated hydrocarbons.

3.7. General Results of the Calculation. To understand the bonding in the Al$_8$C$_6$ core, ab initio (RHF and DFT) calculations were carried out on a modified structure [(AlH)$_6$(AlNH$_3$)$_2$-(CMe)$_6$], optimized under D_{3d} symmetry.[8] The skeleton of the modified structure parallels quite well the main features of the real one. Thus, the computed Al−C bonds of the apical Al atoms are slightly shorter (2.027 Å) than the other ones (2.125 Å). Correspondingly, the Al−C bond orders (0.605 vs 0.523) demonstrate that Al−NR$_3$ units are a bit more tightly bonded to the cluster than are the Al−H ones. Despite different types of Al−C bonds, these can be considered as roughly equivalent throughout the entire cluster, giving a pseudo-octahedral arrangement.

Each carbon atom of the cluster is effectively bonded to four aluminum atoms. This conclusion is supported by the analysis of critical points of electron density,[17] which identifies four points of (3,−1) type around each C atom, on each face of the cube. The complete closure of the bonding network at the surface of the cluster and also the detection of the (3,+3) critical point in the center of the cage indicate that the cluster is of closo type. The structure possesses 12 faces identified by the (3,+1) cycle critical points located in the averaged planes of the Al$_2$C$_2$ fragments, approximately in the middle of the edges of the Al$_8$ cube (see picture in the Supporting Information).

The orbital energy diagram and the orbital shapes suggest that the bonding in the cluster core obeys a pattern related to the octahedral type, irrespective of lower symmetry due to the outer ligands. Consequently, a hypothetical structure with full O_h symmetry was prepared by calculation.[18] This type of calculation was done at the RHF level and was performed with the GAMESS package.[9] This step helps to identify that the different A + E orbital sequences in D_{3d} are originating from corresponding T degenerate representations in O_h (Supporting Information). According to the tensor surface harmonics theory (TSH),[19] the sequence of last occupied MOs, having the $T_{1u} + T_{1g} + T_{2u} + T_{2g}$ representation in O_h, is isomorphous to the set of tangential vector components $P_\pi + \bar{P}_\pi + \bar{D}_\pi + D_\pi$, respectively. For the [(AlH)$_6$(AlNH$_3$)$_2$(CMe)$_6$] cluster, the energies of Kohn−Shamm orbitals (B3LYP and BVWN -DFT calculations) have practically the same order as the canonical RHF ones.

The actual system deviates from the $4n + 2$ electron counting rule of the closo form. The $4n + 2$ rule is valid for clusters with triangular faces (deltahedron) or having four connecting atoms. The distribution of critical points shows that the actual system does not precisely belong to one of these structural types and deviations from the general electron counting rules are possible.[20]

There is a total of 64 electrons comprised in the cluster, suggesting a hypho $4n + 8$ electron count (n = 8Al + 6C =

(17) (a) Bader, R. F. W. *Atoms in Molecules − A Quantum Theory*; Oxford University Press: Oxford, 1990. (b) Bader, R. F. W. *Acc. Chem. Res.* **1985**, *18*, 9−15.

(18) The hypothetical structure with full O_h symmetry can be denoted (Alh*)$_8$-(CC$h^{\#}_4$)$_6$. It was obtained by stressing the formal atoms h* and $h^{\#}$ which possess the same basis set as the proper hydrogen atoms, but having the nuclear charges 1.25 and 0.75, respectively. The supraunitary nuclear charge on h* allows the replacement in the calculation of the nitrogen atoms by hydrides without acquiring a negative charge. In the hypothetical C$h^{\#}_4$ groups, only three electron pairs are involved in the bonding with four point charges (0.75). The C$h^{\#}_4$ object is conceived as a surrogate of a CH$_3$ group, but has the 4-fold symmetry needed for obtaining a true octahedral symmetry (otherwise the CH$_3$ groups located on the faces of a cube are destroying the C_4 axes). The proposed computational experiment of higher symmetry calculation reveals the symmetry parentage of the trigonal structure of the cluster from the octahedral one. This type of calculation was done at the RHF level.

(19) (a) Johnston, R. L.; Mingos, D. M. P. *Theor. Chim. Acta* **1989**, *75*, 11−32. (b) Johnston, R. L.; Zhenyang, L.; Mingos, D. M. P. *New J. Chem.* **1989**, *13*, 33−40. (c) Mingos, D. M. P. *Nature* **1990**, *345*, 113−114. (d) Mingos, D. M. P.; Johnston, R. L. *Struct. Bonding* **1987**, *68*, 29−87. (e) Ceulemans, A.; Mys, G. *Chem. Phys. Lett.* **1994**, *219*, 274−278.

(20) (a) Mingos, D. M. P.; Modrego, J. *New J. Chem.* **1991**, *15*, 9−16. (b) Mingos, D. M. P., Wales, D. J., Eds. *Introduction to Cluster Chemistry*; Prentice Hall Inc.: London, 1990.

14). The cluster itself has 18 electron pairs (excluding the electron pairs within the Al−H and C−C outer bonds). Additionally, there are 24 Al−C atom pairs. Therefore, the Al−C bonds are the subject of a global delocalization. The supplement of three electron pairs does not lead to localized breaking of bonds and generating a hypho cluster, but rather the closo form is preferred due to the stabilization by electron delocalization (hyper-closo type).[21]

3.8. The Actual Bonding Scheme as Surface Aromaticity. The chemical stability of the cluster and the metathesis reactions of the outer groups are comparable with those in aromatic systems. The delocalization of electron density within the cluster allows a number of bonds which is larger than that of available cluster electron pairs. The present case is similar to the surface aromaticity encountered in boranes and carboranes,[22] due to the occurrence of multicenter bonds.

In recent reviews,[23] the idea of aromaticity as a concept is still disputed and judged by different criteria. An indication of aromaticity is given here by the orbital scheme of the Al_4C fragment. This contains a sextet of electrons, accommodated in orbitals with Σ and Π representations in the axial symmetry.

Besides the $4n + 2$ electron count, the orbital definition of aromaticity should be related to a substantial energy stabilization, consistent with a large HOMO−LUMO gap.[24] To obtain a proof, a special treatment was designed, applying a phenomenological model belonging to the type of so-called three-dimensional Hückel[25] (not to be confused with extended-Hückel or simple estimation within traditional Hückel theory). Fitting the corresponding parameters (Supporting Information), a reduced orbital diagram (with 42 levels resulted from three AOs per atom) was adjusted to reproduce the energies resulting from the ab initio calculations.

The ab initio MOs with relevance to the cluster bonding (making the target of fit in the model Hamiltonian) were identified selecting those with the maximal contributions to the Mulliken population of the cluster atoms. The model Hamiltonian was constructed in full octahedral symmetry. Therefore, the fit was taken with respect to the barycenters of orbitals computed in D_{3d} which are originating from the split of higher degeneration in O_h.

A numerical experiment can be performed, starting from the fitted phenomenological Hamiltonian. Scaling with a factor from 0 to 1 all the parameters responsible for orbital interactions between the Al_4C moieties (while keeping the fitted values of parameters acting inside the face), the orbital diagram can be tuned between isolated Al_4C fragments and the whole Al_8C_6 core (Figure 4). In this way, the orbital diagram of the hypothetically separated Al_4C faces is revealed with a large HOMO−LUMO gap (simulated, 11.8 eV). Therefore, the electron sextet combined with an orbital stabilization factor is an indication for the aromatic character on each face. This is a simplified view for the global surface aromaticity.

The Al_4C entities[26] and related systems[27] are known from gas-phase experiments and were also discussed in the perspective of aromaticity. However, due to different electron counting in the orbital scheme, the electronic structure of neutral or ionic Al_4C species is different from that of the Al_4C fragment in the molecule. On the other side, the bonding scheme in the Al_4C fragment may be quite similar to analogous Al_2Zr_2C fragments encountered in $[(Cp^*Zr)_3Al_6Me_8(CH)_5(CH_2)_2]$.[28]

Another interpretation of aromaticity is found in the valence bond (VB) theory.[29] The delocalization of Al−C bonds can be presented as superposition of several equivalent resonance structures.[30,31] The appropriate selection of resonance structures offers a way to design a limited number of states in the configuration interaction problems. The nonstandard formalism of changing the orbital basis is in fact a manner to include contributions of orbital excitations within the orbitals of the central atom parallel to the spin-coupled resonance structures (Supporting Information).

The full lines stand for the electron pairs located in the best overlapping couple of hybrid orbitals (Scheme 3). The dashed ones correspond to bonding through slightly misaligned hybrid orbitals. This representation of the VB resonance structures allows the use of graph theory as a qualitative tool for analyzing the aromatic resonance of the whole cluster. The graph theory was extensively used for the resonance structures of aromatic hydrocarbons[32] or to model various orbital factors in clusters.[33] However, to the best of our knowledge, the enumerating resonance structures for clusters were not developed.

The resonance structures can be represented as a collection of bipartite graphs where the two classes of points are Al and C. These graphs are also edge weighted, the two types of connections corresponding to full and dashed links. Each C vertex is 3-fold connected in all the structures (having one full line and two dashed ones). All the isomers following such definitions can be obtained expanding the polynom given in the Supporting Information.

Among the total number of 4096 structures, 304 are independent types, and only 20 possess symmetry. Figure 5 contains the 20 different configurations possessing nontrivial symmetry. The enumeration and classification of the discussed graphs were

(21) Johnston, R. L.; Mingos, D. M. P.; Sherwood, P. *New J. Chem.* **1991**, *15*, 831−841.
(22) (a) King, R. B. *Chem. Rev.* **2001**, *101*, 1119−1152. (b) von Ragué Schleyer, P.; Najafian, K. *Inorg. Chem.* **1998**, *37*, 3454−3470. (c) von Ragué Schleyer, P.; Najafian, K.; Mebel, A. M. *Inorg. Chem.* **1998**, *37*, 6765−6772.
(23) von Ragué Schleyer, P. *Chem. Rev.* **2001**, *101*, 1115−1117.
(24) De Proft, F.; Geerlings, P. *Chem. Rev.* **2001**, *101*, 1451−1464.
(25) (a) Gimarc, B. M.; Zhao, M. *Inorg. Chem.* **1996**, *35*, 825−834. (b) Zhao, M.; Gimarc, B. M. *Polyhedron* **1995**, *14*, 1315−1325.
(26) (a) Boldyrev, A. I.; Simons, J. *J. Am. Chem. Soc.* **1998**, *120*, 7967−7962. (b) Li, X.; Zhang, H. F.; Wang, L.-S.; Geske, G. D.; Boldyrev, A. I. *Angew. Chem.* **2000**, *112*, 3445−3448; *Angew. Chem., Int. Ed.* **2000**, *39*, 3630−3633.
(27) (a) Wang, L.-S.; Boldyrev, A. I.; Li, X.; Simons, J. *J. Am. Chem. Soc.* **2000**, *122*, 7681−7687. (b) Li, X.; Kuznetsov, A. E.; Zhang, H. F.; Boldyrev, A. I.; Wang, L.-S. *Science* **2001**, *291*, 859−861. (c) Geske, G. D.; Boldyrev, A. I.; Li, X.; Wang, L.-S. *J. Chem. Phys.* **2000**, *113*, 5130−5133. (d) Hirsch, A.; Chen, Z.; Jiao, H. *Angew. Chem.* **2001**, *113*, 2916−2920; *Angew. Chem., Int. Ed.* **2001**, *40*, 2834−2838.
(28) (a) Herzog, A.; Roesky, H. W.; Zak, Z.; Noltemeyer, M. *Angew. Chem.* **1994**, *106*, 1035−1037; *Angew. Chem., Int. Ed. Engl.* **1994**, *33*, 967−968. (b) Herzog, A.; Roesky, H. W.; Jäger, F.; Steiner, A.; Noltemeyer, M. *Organometallics* **1996**, *15*, 909−913.
(29) Klein, D. J., Trinajstiæ, N., Eds. *Valence Bond Theory and Chemical Structure*; Elsevier: Amsterdam, 1990. (b) Gerratt, J.; Cooper, D. L.; Karadakov, P. B.; Raimondi, M. *Chem. Soc. Rev.* **1997**, *26*, 87−100. (c) Cooper, D. L.; Gerratt, J.; Raimondi, M. *Chem. Rev.* **1991**, *91*, 929−964.
(30) (a) Saebo, S.; Pulay, P. *Annu. Rev. Phys. Chem.* **1993**, *44*, 213−236. (b) Schutz, M.; Hetzer, G.; Werner, H. J. *J. Chem. Phys.* **1999**, *111*, 5691−5705.
(31) Raimondi, M.; Cooper, D. L. *Top. Curr. Chem.* **1999**, *203*, 105−120.
(32) (a) Balaban, A. T. *J. Chem. Inf. Comput. Sci.* **1995**, *35*, 339−350. (b) Balaban, A. T. *Pure Appl. Chem.* **1980**, *52*, 1409−1429. (c) Balaban, A. T. *Pure Appl. Chem.* **1982**, *54*, 1075−1096. (d) Trinajstiæ, N. *Chemical Graph Theory*; CRC Press: Florida, 1983.
(33) (a) Johnston, R. L. *Struct. Bonding* **1997**, *87*, 1−34. (b) King, R. B. *Acc. Chem. Res.* **1992**, *25*, 247−253. (c) King, R. B.; Dai, B.; Gimarc, B. M. *Inorg. Chim. Acta* **1990**, *167*, 213−222.

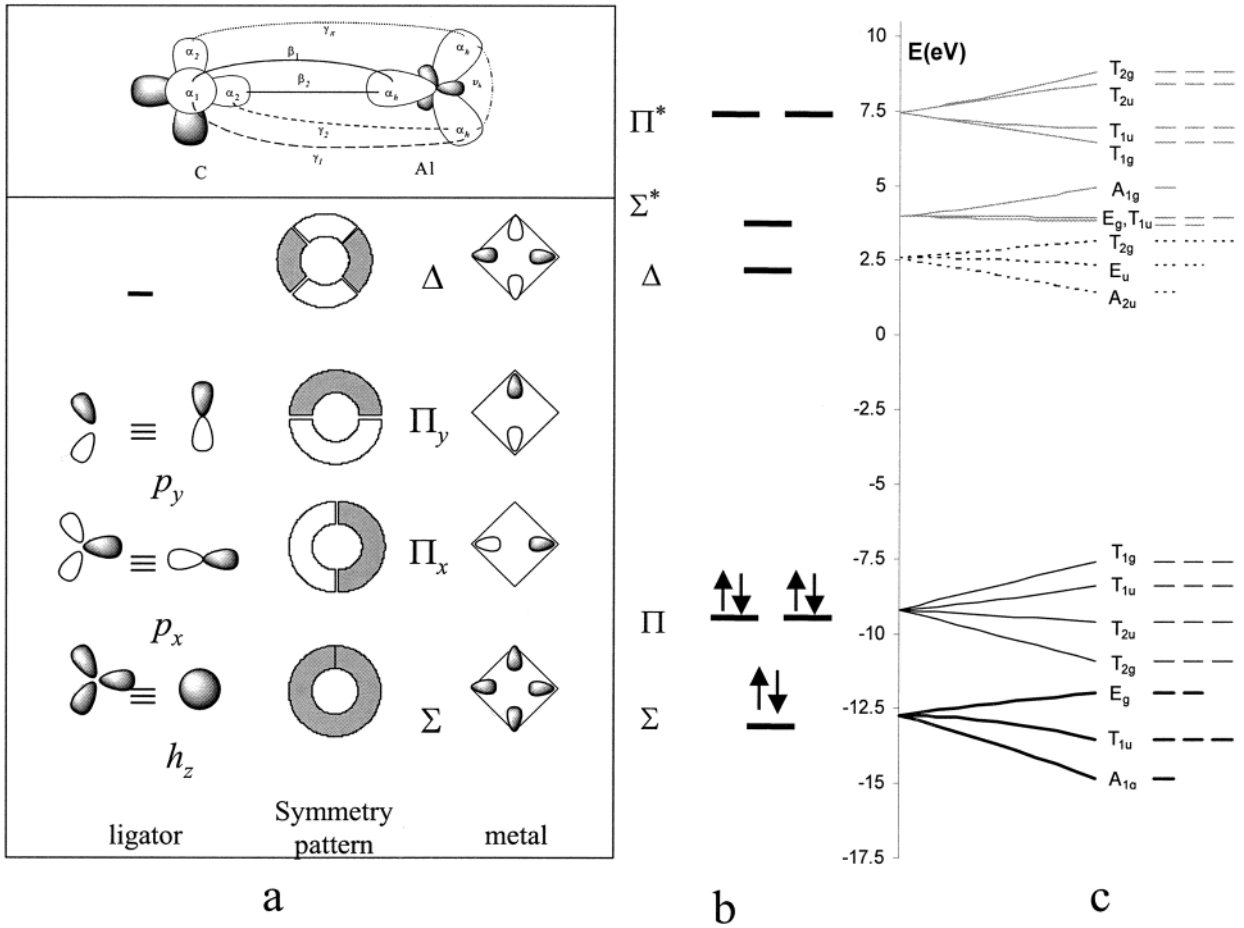

Figure 4. (a) The orbital symmetries, (b) the simplified model of the bonding of one Al_4C face, and (c) the full three-dimensional Hückel simulation of cluster orbitals. Panel (a) evidences the axial symmetry correspondence between C and Al_4 orbitals as well as the equivalence between hybrid or the pure AO scheme on carbon. The component denoted h_z is a sp_z based hybrid, directed toward the Al_4 face. The occupancy and symmetry of the MOs suggest an aromatic-type sextet pattern (b). The HOMO−LUMO of one Al_4C is simulated to be large by means of hypothetical quenching of the interaction terms from the full cluster Hamiltonian. The effective Hamiltonian is constructed in a three-dimensional Hückel model and is fitted to reproduce occupied levels from the ab initio MO scheme.

Scheme 3

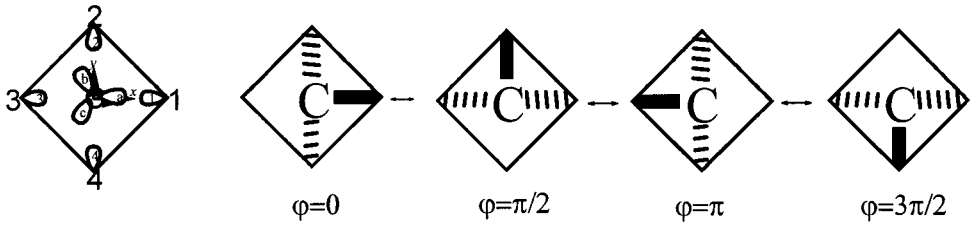

done by automatic computer generated structures. For the whole cluster, the VB approach is prohibitive for a direct quantum calculation, whereas the graph theory allows a valuable qualitative handling. Various semiquantitative measures for aromaticity can be generally resumed with the index named topological resonance per electron (TREPE).[34] In our case, the three-dimensional Hückel modeling given previously was used for such an estimation.

The actual estimation of TREPE indices is given below the corresponding graphs presented in Figure 5. The relatively high values (eV) are due to the fact that delocalization acts upon quite strong σ bonds. The narrow distribution of TREPE indices for all the isomers around the average value suggests that despite topological differentiation, all the possible structures contribute comparably to the overall resonance.

4. Conclusions

Altogether, we presented a facile synthesis for new carbaalanes and their chlorinated derivatives including a functionalization of the inner and outer sphere of the cluster. This is also a route to RCH_2C^{3-} carbanions, which are only connected to electropositive aluminum atoms and stabilized without using electron-withdrawing groups. The ^{13}C NMR of the cluster carbon is shifted to lower field as compared to that of other organo aluminum compounds. This is tentatively assigned to aromatic-NMR correlation, for a group placed inside of the ring

(34) (a) Dewar, M. J. S.; de Llano, C. *J. Am. Chem. Soc.* **1969**, *91*, 789−795. (b) Graovac, A.; Gutman, I.; Randiæ, M.; Trinajstić, N. *J. Am. Chem. Soc.* **1973**, *95*, 6267−6273. (c) Aihara, J.-I. *J. Am. Chem. Soc.* **1977**, *99*, 2048−2053. (d) Aihara, J.-I. *J. Am. Chem. Soc.* **1995**, *117*, 4130−4136. (e) Katritzky, A. R.; Jug, K.; Oniciu, D. C. *Chem. Rev.* **2001**, *101*, 1421−1449. (f) Schaad, L. J.; Andes Hess, B., Jr. *Chem. Rev.* **2001**, *101*, 1465−1476.

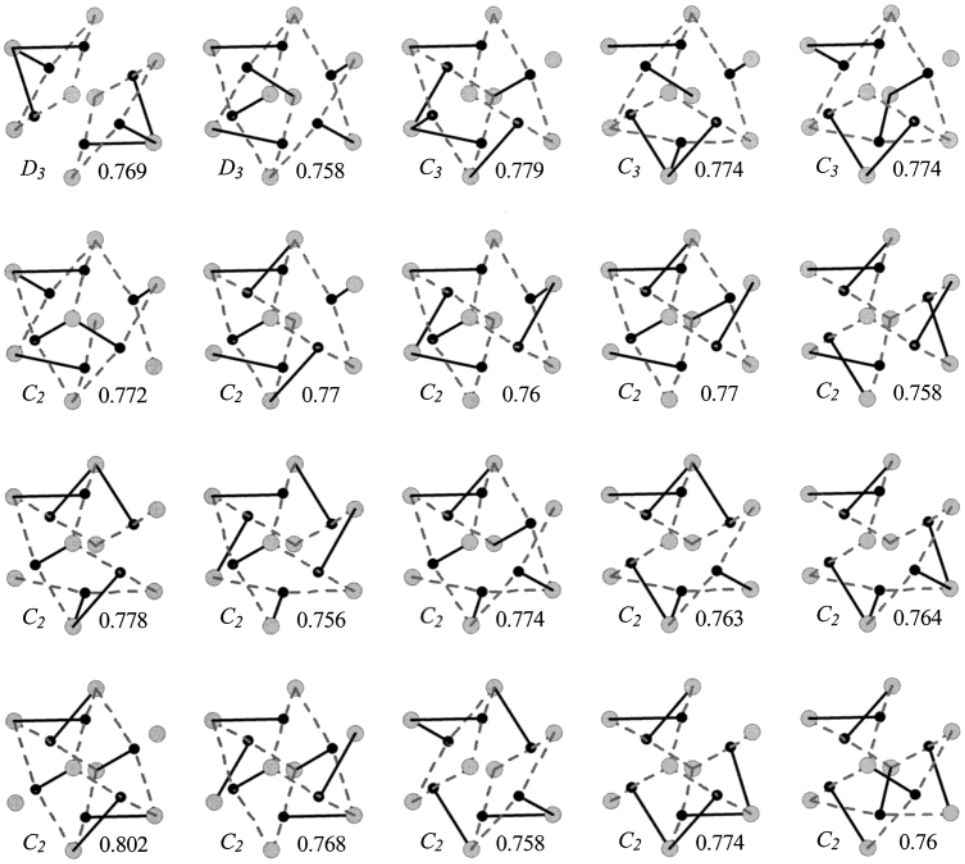

Figure 5. The graphs possessing nontrivial symmetry among the 304 different species possible for qualitative enumeration of VB structures of the Al_8C_6 cluster. The bipartite graph contains edges only between Al and C species, weighted by two types of connections. The full lines suggest spin-coupling between a C hybrid, fully directed to the Al hybrid, while the dashed lines correspond to a coupling between metal and ligand lobes deviated by 30° with respect to the axial directions of the Al_4C pyramids.

current. The ^{1}H NMR is practically not influenced due to the relatively large separation from the Al_4 rings. The high stability of the cluster core is demonstrated by its chemistry and proved by calculations.

The pseudo-octahedral nature of the bonding scheme was proven by ab initio calculations and further modeling. The orbital levels of the D_{3d} cluster are regarded as relatively small splitting of the octahedral parents. The lowered trigonal symmetry of the cluster is exclusively due to the outer ligands which are not essentially influencing the bonding in the Al_8C_6 core.

The multicenter bonding implies a global delocalization introducing the three-dimensional aromaticity for the actual bonding scheme. For the Al_4C fragment, a sextet with large HOMO−LUMO separation is found. A semiquantitative proof was developed modeling the cluster orbitals. The corresponding parameters were obtained by a fit to the ab initio MOs. The same model allowed to estimate the topological resonance index (TREPE) applied to the resonance isomers obtained by computer enumeration of the corresponding graphs. Valence bond arguments were used also to substantiate the idea of face and surface aromaticity in the given class of clusters. The idea of aromaticity used in clusters and organometallic chemistry could lead to a new concept in preparative chemistry.

Acknowledgment. This work is dedicated to Professor George M. Sheldrick. This work was supported by the Deutsche Forschungsgemeinschaft and the Göttinger Akademie der Wissenschaften. M.F. is grateful to the Alexander von Humboldt Foundation for a research fellowship. We are grateful to Dr. N. Dragoe (Tokyo University) for technical assistance in using Gaussian 98.

Supporting Information Available: Crystallographic material of the presented structures, CIF files, and a detailed description of the phenomenological modeling of MO scheme, VB considerations, and graph theoretical methods (PDF). This material is available free of charge via the Internet at http://pubs.acs.org.

JA012035K